Nonlinear Controller for Induction Motor Drive

K. B. Mohanty*
Department of Electrical Engineering
IIT Kharagpur-721302, India

N. K. De
Department of Electrical Engineering
IIT Kharagpur-721302, India

Abstract—**An attempt has been made in the present work to improve the dynamic and steady state performances of the vector controlled induction motor (IM) drives. Input-output linearization and decoupling technique based on the concepts of differential geometry, has been used to decouple the speed, or torque from flux. Optimal proportional-integral (P-I) controllers in flux and speed loops are designed to obtain desired dynamic and steady state responses. A new rotor flux observer has been designed to estimate the flux at all speeds. Simulation results show that the performance of the drive system with the designed controller is comparable to that with vector controller and the proposed drive system is more flexible.**

Keywords: Induction motor drive, Vector control, Input-output linearization, Input-output decoupling, P-I controller, Reduced order observer, Flux estimation.

I. INTRODUCTION

The industrial standard for high performance motion control applications requires four-quadrant operation, including field weakening, minimum torque ripple, rapid speed recovery under impact load torque in addition to fast dynamic torque and speed responses. DC motor drives, though fulfilling the needs, are handicapped by problems arising out of commutation requirements in addition to low torque-to-weight ratio and reduced unit capacity. Induction Motors (IM) are suitable for industrial drives, because of their simple and robust structure, higher torque-to-weight ratio, higher reliability and ability to operate in hazardous environment. However, their control is a challenging task, because the rotor current, responsible for the torque production, is induced from the stator current and also contributes to net air-gap flux resulting in coupling between torque and flux. The constant voltage to frequency ratio (V/f) control scheme has become the simplest, cheapest, and thus, most common choice amone the scalar control methods for speed control of IM, where the transient performance is not critical. The control of IM in field coordinates using vector control (also known as field oriented control) as proposed by Blaschke [1] and Hasse [2], leads to decoupling between the flux and torque, thus, resulting in improved dynamic torque and speed responses. Significant advances have been made in vector control of induction motors since then. Vector control of an ac motor is possible with respect to any arbitrary flux vector (stator, rotor or air-gap) by proper orientation of the armature current vector using a decoupling network.

A universal field oriented controller has been developed [3] for an IM to achieve decoupling between flux and torque in any arbitrary flux reference frame and the corresponding decoupling network has been designed, both for flux feedback (direct) [1] and flux feedforward (indirect) [2] methods. Rotor flux orientation scheme has advantages over stator or air-gap flux orientation schemes, as complete decoupling of flux and torque is obtained without any additional decoupling network. Indirect field orientation scheme has certain advantages over direct field orientation scheme for drives run at low speeds.

A disadvantage of the field-oriented controller [1] is that the method assumes that the magnitude of the rotor flux is regulated to a constant value. Therefore, the rotor speed is only asymptotically decoupled from the rotor flux. The concepts of differential geometry [4,5] have found considerable use in the development of control techniques for multivariable nonlinear systems. Such schemes have resulted in solutions to several problems, including feedback linearization, input-output linearization and decoupling, and disturbance decoupling. Following Krzeminski [6], Marino et. al. [7] developed a voltage command input-output linearization controller, which decouples the rotor flux and speed, based on a nonlinear transformation performed on the state variables. Kim et. al. [8] have reported a current command input-output linearization controller. A new approach is presented in this paper based on [4-8] for input-output linearization and decoupling control of induction motor, and also to improve the dynamic torque and speed responses for high performance motion control applications.

In section II, the induction motor model, suitable for rotor flux orientation scheme is presented. The model is then simplified for alignment of d-axis with the rotor flux. The IM model is linearized by using input-output linearization technique, in section III. Linear controllers are synthesized to obtain good dynamic and steady state responses. In section IV, the rotor flux is estimated from the measured values of terminal voltages and currents. Gopinath's reduced order observer [11-12] has been extended to estimate the rotor flux, accurately at all speeds. Simulation results are discussed in section V.

II. INDUCTION MOTOR MODEL

From the voltage equations of the induction motor in the synchronously rotating d-q axes reference frame, the state space model with stator current and rotor flux components as state variables as derived in [8] is given as:

* On QIP study leave from REC, Rourkela

0-7803-5812-0/00/$10.00©2000IEEE

$$\begin{bmatrix} \dot{i}_s \\ \dot{\Psi}_r \end{bmatrix} = \begin{bmatrix} A_{11} & A_{12} \\ A_{21} & A_{22} \end{bmatrix} \begin{bmatrix} i_s \\ \Psi_r \end{bmatrix} + \begin{bmatrix} B_1 \\ 0 \end{bmatrix} v_s \quad (1)$$

where, $i_s = \begin{bmatrix} i_{ds} & i_{qs} \end{bmatrix}^T$, $\Psi_r = \begin{bmatrix} \Psi_{dr} & \Psi_{qr} \end{bmatrix}^T$,

$v_s = \begin{bmatrix} v_{ds} & v_{qs} \end{bmatrix}^T$,

$A_{11} = -a_1 I - \omega_e J$, $A_{12} = a_2 I - P a_3 \omega_r J$,

$A_{21} = a_5 I$, $A_{22} = -a_4 I - (\omega_e - P\omega_r) J$, $B_1 = c I$.

$I = \begin{bmatrix} 1 & 0 \\ 0 & 1 \end{bmatrix}$, $J = \begin{bmatrix} 0 & -1 \\ 1 & 0 \end{bmatrix}$.

$c = L_r / (L_s L_r - L_m^2)$,

$a_1 = c R_s + c R_r L_m^2 / L_r^2$, $a_2 = c R_r L_m / L_r^2$,

$a_3 = c L_m / L_r$, $a_4 = R_r / L_r$, $a_5 = R_r L_m / L_r$.

where,

R_s , R_r , L_s , L_r , L_m : Motor parameters (given in appendix).

P : Number of pole pairs,

ω_r : Mechanical rotor angular velocity,

ω_e : Fundamental supply frequency,

v_{ds} , v_{qs} : d-q axes stator phase voltages,

i_{ds} , i_{qs} : d-q axes stator phase currents,

Ψ_{dr} , Ψ_{qr} : d-q axes rotor fluxes.

The torque developed by the motor is

$$T_e = K_t (\Psi_{dr} i_{qs} - \Psi_{qr} i_{ds}) \quad (2)$$

where,

$K_t = 3 P L_m / 2 L_r$

The conditions required for decoupling control [9] are

$\Psi_{qr} = 0$ and $\dot{\Psi}_{qr} = 0$

From (1),

$\dot{\Psi}_{qr} = a_5 i_{qs} - (\omega_e - P\omega_r) \Psi_{dr} - a_4 \Psi_{qr}$

Decoupling is obtained, when

$a_5 i_{qs} = (\omega_e - P\omega_r) \Psi_{dr}$

or, $\omega_e = P\omega_r + a_5 i_{qs} / \Psi_{dr}$ (3)

When (3) is satisfied, the dynamic behaviour of the induction motor after sufficient time is given by:

$$\dot{i}_{ds} = -a_1 i_{ds} + a_2 \Psi_{dr} + \omega_e i_{qs} + c v_{ds} \quad (4)$$

$$\dot{i}_{qs} = -\omega_e i_{ds} - a_1 i_{qs} - P a_3 \omega_r \Psi_{dr} + c v_{qs} \quad (5)$$

$$\dot{\Psi}_{dr} = -a_4 \Psi_{dr} + a_5 i_{ds} \quad (6)$$

The developed torque, $T_e = K_t \Psi_{dr} i_{qs}$ (7)

Even in the IM model described by (4)-(7), nonlinearity and interaction exist.

III. CONTROLLER DESIGN

A. *Input-Output Linearization*

The concept behind field oriented control is that rotor flux can be controlled according to (6), with i_{ds} acting as the control input. The q-axis current component i_{qs} serves as an input in order to control the torque (7) as a product of ψ_{dr} and i_{qs}. But transition from field oriented voltage components, v_{ds} and v_{qs} to current components as in (4) and (5) involves leakage time constants and interactions. The interaction between current components and nonlinearity in the overall system are eliminated by using the input-output linearization approach [4-8].

Let the developed torque, T_e be chosen as a variable in place of i_{qs} in the induction motor model. Differentiating both sides of (7) and simplifying with appropriate substitutions:

$$\dot{T}_e = -(a_1 + a_4) T_e + K_t \Psi_{dr} \left[c v_{qs} - P \omega_r (i_{ds} + a_3 \Psi_{dr}) \right] \quad (8).$$

The nonlinear control laws are chosen as

$$u_1 = \omega_e i_{qs} + c v_{ds} \quad (9)$$

$$u_2 = K_1 \Psi_{dr} \left[c v_{qs} - P \omega_r (i_{ds} + a_3 \Psi_{dr}) \right] \quad (10)$$

The induction motor model is now decoupled into two linear subsystems: (1) electrical and (2) mechanical.

(1) Electrical subsystem:

$\dot{i}_{ds} = -a_1 i_{ds} + a_2 \Psi_{dr} + u_1$

$\dot{\Psi}_{dr} = -a_4 \Psi_{dr} + a_5 i_{ds}$

(2) Mechanical subsystem:

$\dot{T}_e = -(a_1 + a_4) T_e + u_2$

$\dot{\omega}_r = (T_e - T_l - B\omega_r) / J$

The transformed model given above is valid only for $\psi_{dr} \neq 0$. Since the induction motor system described by the above four equations is linear and decoupled, the developed torque (or the speed) and the rotor flux are independently controlled. Linear control theories are used to obtain desired steady state and transient performance. Here, the linearizing control inputs, u_1 and u_2 are derived using Proportional-Integral (P-I) controllers. The block diagrams of the electrical and mechanical subsystems with P-I controllers are shown in Figures 1-3.

B. *Design of P-I Controllers*

The electrical subsystem with one P-I controller is shown in Fig. 1. The mechanical subsystem with one P-I controller is shown in Fig. 2, and that with two P-I controllers is shown in Fig. 3. One P-I controller in the electrical or mechanical subsystem is used due to simplicity of the control law. In the electrical subsystem, one P-I controller is adequate for good dynamic response. The necessity of two P-I controllers in the mechanical subsystem, arises because of significant difference in the time constants of the speed and current, or electromagnetic torque. This is verified by the simulation results. In the following figures and derivations, K_{p1}, K_{p2}, K_{p3}, K_{p4} are the gains of the proportional controllers and K_{i1}, K_{i2}, K_{i3}, K_{i4} are the gains of the integral controllers.

In the present drive system, the open loop transfer function of the linearized electrical subsystem (refer Fig. 1)

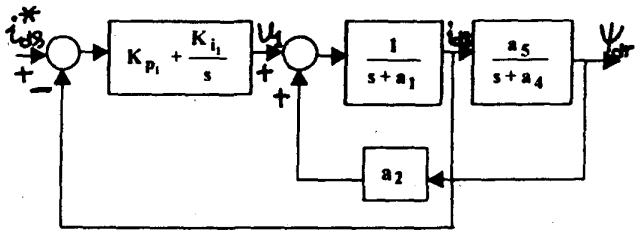

Figure. 1. Block diagram of the closed-loop electrical subsystem

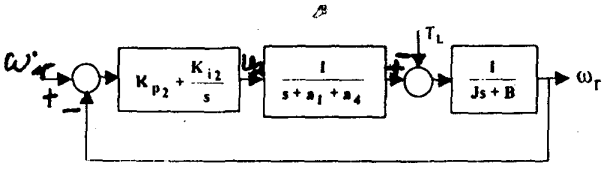

Fig. 2. Mechanical subsystem with one P-I controller

$$\frac{i_{ds}(s)}{u_1(s)} = \frac{s + a_4}{s^2 + (a_1 + a_4)s + (a_1 a_4 - a_2 a_5)}$$

has two poles at -10.22 and -288.55 (corresponding to motor parameters given in the appendix).

Let $K_{i1} = 288.55\ K_{p1}$, so that the pole at -288.55 is cancelled by the zero of the P-I controller. Then, the closed loop transfer function is,

$$\frac{i_{ds}(s)}{i^*_{ds}(s)} = \frac{K_{p1}(s + a_4)}{s^2 + (10.22 + K_{p1})s + K_{p1} a_4}$$

Let K_{p1} a4 = 2500, corresponding to a natural frequency of 50 rad/s. Then, the designed values of K_{p1} and K_{i1} are obtained as 151.27 and 43649, respectively.

From Fig. 2, the closed loop transfer function of the mechanical subsystem is,

$$\frac{\omega_r(s)}{\omega^*_r(s)} = \frac{K_{p2}s + K_{i2}}{Js^3 + d_2 s^2 + d_1 s + K_{i2}}$$

where,

$d_1 = B(a_1 + a_4) + K_{p2}$; $d_2 = J(a_1 + a_4) + B$.

To achieve good transient response, modulus optimum method [10] is used. The controller gains are,

$d_1 = d_2^2 / 2J = 393$.

So, $K_{p2} = 393$.

$K_{i2} = d_1^2 / 2 d_2 = 29340$.

To improve the dynamic response of torque and speed further, two P-I controllers are used in the mechanical subsystem as shown in Fig. 3.

Let $K_{i3} = (a_1 + a_4)\ K_{p3}$, so that the pole at $-(a_1 + a_4)$ is cancelled by the zero of the P-I controller. If K_{p3} is chosen as 100, the torque response is instantaneous. So, the closed loop transfer function of the inner loop is taken as unity. Then, the overall closed loop transfer function of the mechanical subsystem can be expressed as:

$$\frac{\omega_r(s)}{\omega^*_r(s)} = \frac{K_{p4}\,s + K_{i4}}{Js^2 + (B + K_{p4})s + K_{i4}}$$

For the above second order system, taking the natural frequency and damping coefficient to be 15 rad/s and 1.0, the values of K_{p4} and K_{i4} are found to be 0.261 and 1.98 respectively [10].

IV. ESTIMATION OF ROTOR FLUX

The value of rotor flux, ψ_{dr} is used to compute the control inputs (3), (9) and (10). However, it is difficult to measure the rotor flux in an induction motor. Therefore, the rotor flux is estimated using the measured values of speed, stator current and voltage. Gopinath's reduced order observer [11,12] is extended to estimate the rotor flux.

From the second row of (1), the flux observer equation with an error correction term is derived as follows:

$$\dot{\hat{\Psi}}_r = A_{21} i_s + A_{22} \hat{\Psi}_r + G\left[\, \dot{i}_s - (A_{11} i_s + A_{12} \hat{\Psi}_r + B_1 v_s) \,\right] \qquad (11)$$

where, $\hat{\Psi}_r$ is the estimated rotor flux and G is the gain matrix.

For this observer, the flux error dynamics is,

$$\dot{\tilde{\Psi}}_r = (A_{22} - G A_{12})\ \tilde{\Psi}_r . \qquad (12)$$

where, error in the is estimate, $\tilde{\Psi}_r = \Psi_r - \hat{\Psi}_r$.

Since the induction motor system is observable, the eigenvalues of $(A_{22} - G A_{12})$ matrix are assigned at the desired locations by choosing suitable gain matrix, G.

In order to eliminate the differential term of current in (11), a new variable,

$$\hat{\xi} = \hat{\Psi}_r - G i_s \qquad (13)$$

is substituted into (11), which after simplification comes out as:

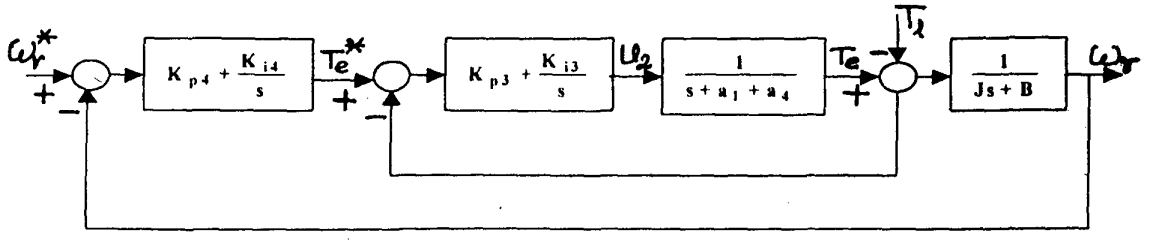

Fig. 3. Mechanical subsystem with two P-I controllers

$$\dot{\hat{\xi}} = (A_{22} - GA_{12})\hat{\xi} - G B_1 \cdot v_s + \left[A_{21} - G A_{11} + (A_{22} - G A_{12})G\right] \cdot i_s \quad (14)$$

To place the eigenvalues of $(A_{22} - G A_{12})$ at $(-x \pm j y)$ rad/s, the observer gain matrix, G is given by $(g_1 I + g_2 J)$, where,

$$g_1 = \frac{(x - a_4)\, a_2 + (y + \omega_e - P\omega_r)\, Pa_3\omega_r}{a_2^2 + (Pa_3\omega_r)^2}$$

$$g_2 = \frac{(x - a_4)\, Pa_3\omega_r - (y + \omega_e - P\omega_r)\, a_2}{a_2^2 + (Pa_3\omega_r)^2}$$

The rotor flux is estimated by solving for $\hat{\xi}$ from (14) and then from (13) as, $\hat{\Psi}_r = \hat{\xi} + G i_s$.

V. SIMULATION RESULTS AND DISCUSSIONS

The drive system with the controller and observer has been simulated using MATLAB. Some of the simulation results along with the comments are presented below.

(A) Reference speed is increased from 1000 r/min to 1300 r/min and then decreased to 800 r/min after 1 second. Reference flux linkage and load torque are kept constant at 0.45 V·s and 1 N·m. The simulation results are shown in Fig. 4. Fig. 4 (a) shows the speed response. Fig. 4 (b) shows the flux linkage and the estimated value of flux linkage. As seen from these figures, the settling time and overshoots are well within acceptable limits. The mechanical speed has a peak undershoot of 10% momentarily for about 0.2 seconds, when the step decrease in the speed command is 500 r/min. The overshoot in the flux linkages is 3.8% in that case, which is very small and indicates that the machine operates with almost constant flux. The flux observer estimates the flux with a little error, only during the transient period. The flux observer is insensitive to speed variations.

(B) To test the performance of the drive with load-torque disturbances, the load has been increased from 1 N·m to 4 N·m and then decreased to 2 N·m after 1.0 second. The speed and flux linkage commands are kept at their nominal values, 1000 r/min and 0.45 V·s respectively. Fig. 5 depicts the speed and d-q axes stator currents. As can be seen from these figures, the maximum speed fluctuation is within 100 r/min momentarily (for about 0.2 seconds). The flux component of the stator current remains constant at its nominal value and the torque component of the current changes according to the load disturbances. The overshoot in the currents is minimal showing no sudden spikes in supply current, which would have led to voltage dip and other undesirable phenomena at the dc link to which the motor is connected.

(C) To test the drive in the constant power mode for operation above the base speed region, the following test has been carried out. At a constant load torque of 4 N·m, the speed is increased from 1000 r/min to 1500 r/min (base speed), at a reference flux linkage of 0.45 V·s, and then to 1800 r/min with flux weakening. The speed and flux responses are shown in Fig. 6 (a) and Fig. 6 (b), respectively. As can be seen, the rotor flux almost settles at the new value (0.375 V·s) very quickly. The speed change also shows small overshoot (2.8%).

The above results show that flux and speed are completely decoupled. Instantaneous speed response is achieved, while flux remains almost constant at the set value. Estimated flux follows the actual flux closely. As a current controller is used in the electrical subsystem, the d-axis stator current remains constant, under all circumstances (refer Fig. 5 (b)). The objective of vector control is achieved, when the motor is fed from a Voltage Source Inverter (VSI). Fast torque response is another advantage of this system.

The proposed control system is being implemented using a PC-based system. The induction motor is supplied from a VSI. The analog signals, such as rotor position, terminal voltages and currents, are interfaced to the PC by means of a data acquisition card (PCL-208). The complete control algorithm, including the coordinate transformation, is to be implemented by software in an 80486-based PC. Digital to Analog Converter (DAC) card (PCL-726) is to be used to provide the analog command frequency and voltage to the inverter control circuit. The experimental set-up is currently under fabrication in the laboratory.

VI. CONCLUSION

A controller for induction motor drive using input-output linearization and decoupling technique is developed. This is an improvement of rotor flux feedforward vector controller. Proportional-integral (P-I) controllers are used to control the dynamic and steady state responses of flux, speed, torque or current, independent of each other. A reduced order observer is also designed to estimate the rotor flux at all speeds. The simulation results show that the dynamics are controlled in about 0.2 second, fast for such systems, and also the voltage and current variations are within limits. Overshoot in speed and developed torque are also within limits. The implementation is underway in the laboratory.

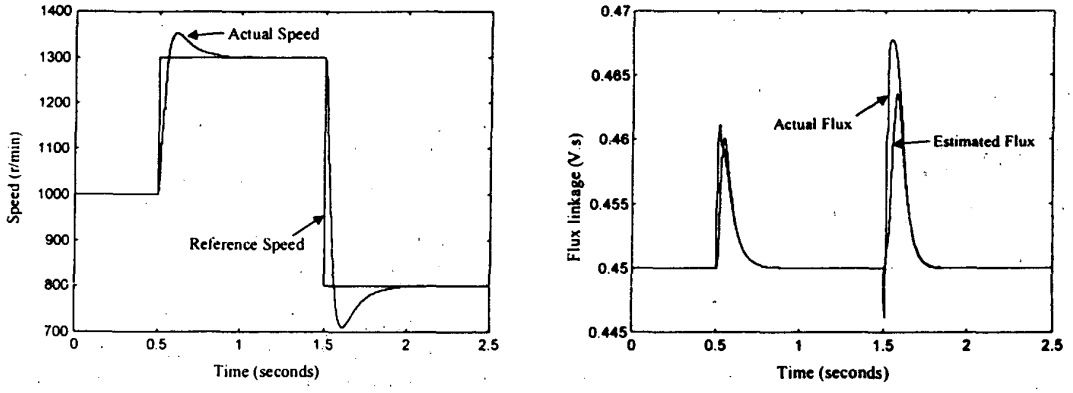

(a) (b)

Fig. 4 Step changes in speed command (a) speed response, (b) estimated and actual flux linkage

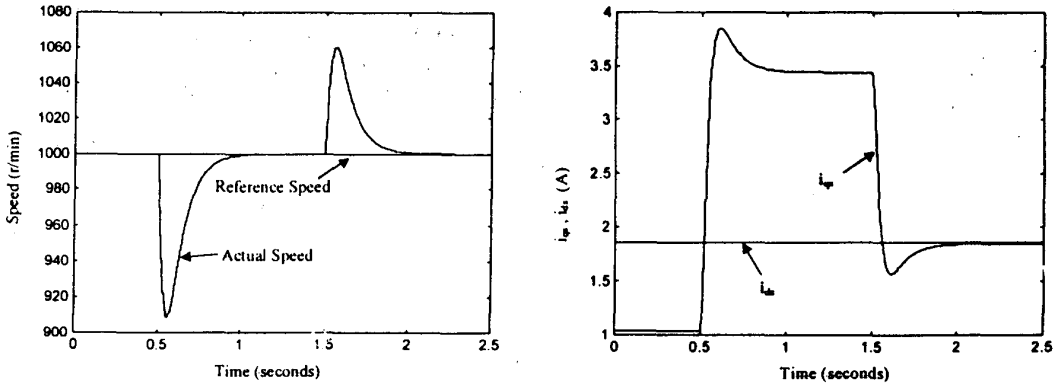

(a) (b)

Fig. 5 Step changes in load torque: (a) speed response, (b) d-q axes stator currents

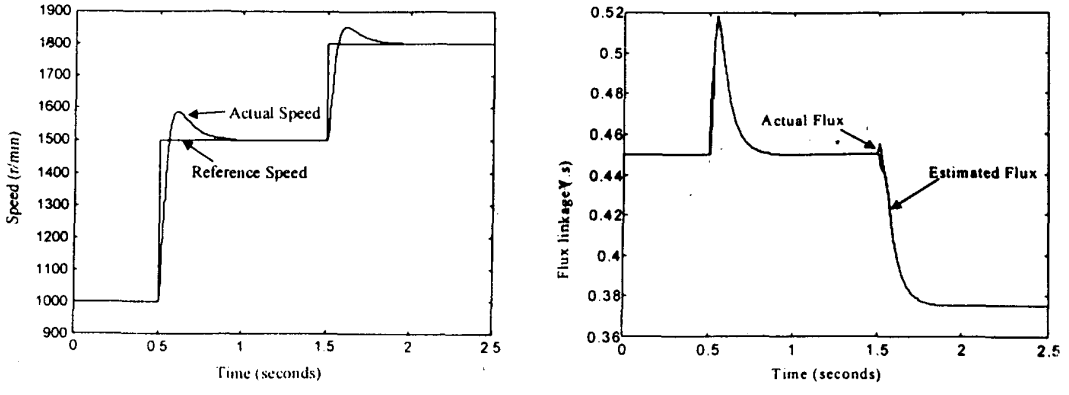

(a) (b)

Fig. 6 Step changes in speed command with flux weakening above base speed: (a) speed response, (b) flux linkage.

VII. APPENDIX

Rating and parameters of the induction motor are:
0.75 kW, 3-phase, 220 V, 3 A, 50 Hz, 1440 r/min
Stator resistance, $R_s = 6.37\ \Omega$
Rotor resistance, $R_r = 4.3\ \Omega$
Mutual inductance, $L_m = 0.24$ H
Stator/Rotor leakage inductance = 0.02 H
Stator/Rotor self-inductance, L_s, $L_r = 0.26$ H
Moment of inertia (motor + load), $J = 0.01\ kg{\cdot}m^2$
Damping coefficient, $B = 0.003\ N{\cdot}m{\cdot}s/rad$

VIII. REFERENCE

[1] F. Blaschke, "The principle of field orientation as applied to the new TRANSVEKTOR closed-loop control system for rotating-field machines,". Siemens Review, vol. 39, no. 5, May 1970, pp. 217-220.

[2] K. Hasse, "On the dynamic behavior of induction machines driven by variable frequency and voltage source," ETZ Arch. Bd. 89, H. 4, 1968, pp. 77-81.

[3] R. W. De Doncker, and D. W. Novotny, "The universal field oriented controller," IEEE Trans. on Industry Applications, vol. 30, no. 1, February 1994, pp. 92-100.

[4] A. Isidori, A. J. Krener, C. Gori-Giorgi, and S. Monaco, "Nonlinear decoupling via feedback: A differential-geometric approach," IEEE Trans. on Automatic Control, vol. 26, 1981, pp. 331-345.

[5] T. J. Tarn, A. K. Bejczy, A. Isidori and Y. Chen, "Nonlinear feedback in robot arm control," Proceedings of 23rd Conference on Decision and Control, December 1984, pp.736-751, CH2093-3/84.

[6] Z. Krzeminski, "Nonlinear control of induction motor," IFAC 10th World Congress on Automatic Control, vol. 3, Munich, 1987, pp. 349-354.

[7] R. Marino, S. Peresada, and P. Valigi, "Adaptive input-output linearizing control of induction motors," IEEE Trans. on Automatic Control, vol. 38, no. 2, 1993, pp. 208-221.

[8] G. S. Kim, I. J. Ha and M. S. Ko, "Control of induction motors for both high dynamic performance and high-power efficiency," IEEE Trans. on Industrial Electronics, vol. 39, no. 4, Aug. 1992, pp. 323-333.

[9] B. K. Bose, *Power Electronics and AC Drives*, Englewood Cliffs, NJ: 1986, p. 272.

[10] K. J. Astrom and T. Hagglund, *PID Controllers: Theory, Design, and Tuning*, Second Edition, Instrument Society of America, The International Society for Measurement and Control, 1995, p. 166.

[11] B. Gopinath, "On the control of linear multiple input-output systems," The Bell System Technical Journal, vol. 50, no. 3, March 1971, pp. 1063-1081.

[12] Y. Hori, V. Cotter, and Y. Kaya, "Control theoretical considerations relating to an induction machine flux observer," IEE Proc., vol. 106-B, 1986, pp. 1001-1008.